Magnetic states of transition metal impurities in silicon carbide

2009 J. Phys.: Condens. Matter 21 206004

(http://iopscience.iop.org/0953-8984/21/20/206004)

J. Phys.: Condens. Matter **21** (2009) 206004 (11pp) doi:10.1088/0953-8984/21/20/206004

Magnetic states of transition metal impurities in silicon carbide

Andrei Los[1,2,3] **and Victor Los**[3]

[1] ISS Ltd, Semiconductors and Circuits Lab, 15 Bozhenko Street, 03680 Kiev, Ukraine
[2] Freescale Semiconductor Incorporated, 15 Bozhenko Street, 03680 Kiev, Ukraine
[3] Institute of Magnetism, 36-b Vernadsky Boulevard, 03142 Kiev, Ukraine

E-mail: andrei.los@freescale.com

Received 27 January 2009, in final form 26 March 2009
Published 24 April 2009
Online at stacks.iop.org/JPhysCM/21/206004

Abstract
Electronic properties of 3C silicon carbide with substitutional transition metal impurities are calculated using an *ab initio* full-potential linearized augmented plane wave technique. It is shown that transition metal atoms in an SiC host may exist in both magnetic and nonmagnetic states. For different impurity species, the transition from the nonmagnetic to the magnetic state and the corresponding change of the atomic magnetic moments may take place either gradually as the volume of the unit cell changes or when the energy gap between the two states is overcome. The magnetic and nonmagnetic solutions are characterized by significantly different unit cell geometries, which are analysed in detail. Magnetic ordering is studied for a number of transition metal impurities in SiC and mean-field estimates of the Curie temperature are given. Calculated densities of states are used to analyse the nature of the exchange interaction between the impurities. Some properties of transition metal impurities are compared for 3C and 4H silicon carbide substitution.

(Some figures in this article are in colour only in the electronic version)

1. Introduction

Considerable research effort has been invested in the past decade into investigations of magnetic properties of diluted magnetic semiconductors (DMS). It is expected that a semiconductor matrix with several per cent of substitutional transition metal (TM) impurities ordered ferromagnetically could serve as a source or filter of spin-polarized carriers in new functional spin-electronic devices [1–3]. Various material systems have been considered as possible candidates for DMS applications. The most studied and well-understood DMS material is (Ga, Mn)As, where significant progress has been achieved in increasing ferromagnetic ordering temperature. Still, however, the reported value of the Curie temperature of 180 K [4] is not sufficiently high for most practical applications. The mean-field theory of ferromagnetism by Dietl *et al* [5, 6] had created a great deal of interest in magnetic properties of wide bandgap semiconductors. The theory predicted that above room temperature carrier-mediated ferromagnetism may be realized in certain wide bandgap compounds, including a family of III-nitrides and ZnO. Apparent early successes in fabricating DMS samples exhibiting ferromagnetism above room temperature [7, 8], attributed to the formation of homogeneous DMS alloys, were in many cases later explained by other effects, such as impurity clustering, at the time overlooked by standard characterization techniques. Much theoretical understanding has been gained since then on the effects of exchange interaction, self-compensation, spinodal decomposition, etc. Given that various effects may mimic a 'true DMS' behaviour, a careful investigation of the microscopic picture of magnetic moments formation and their interaction is required for a realistic prediction of the properties of this complicated class of materials.

Silicon carbide is another wide bandgap semiconductor which has been considered a possible candidate for spin electronics applications. SiC has a long history of materials research and device development and has already been commercialized for high-frequency and high-power applications[1]. SiC exists in a large number of crystal lattice modifications or polytypes and has excellent transport and dopability properties [9]. The mean-field theory [5]

[1] Cree Incorporated, 4600 Silicon Drive, Durham, NC 27703, USA.

predicted that semiconductors with light atoms and smaller lattice constants might possess stronger magnetic coupling and larger ordering temperatures. Although not applied directly to studying magnetic properties of SiC, these predictions make SiC DMS a promising candidate for spintronics applications. Relatively little attention has been paid to the investigation of magnetic properties of SiC doped with TM impurities, and the results obtained so far are rather contradictory. A ferromagnetic response was observed experimentally in Ni-, Mn-and Fe-doped SiC with the values of the Curie temperature T_C varying from significantly below to close to room temperature. The authors assigned the magnetic signal to either the true DMS behaviour [10, 11] or to secondary phase formation [11, 12]. Recent experimental studies of Cr-doped SiC reported this material to be ferromagnetic with the $T_C \sim 70$ K for Cr concentration of ∼0.02 wt% [13], while above room temperature magnetism with varying values of the atomic magnetic moments was observed for Cr concentrations of 7–10 at.% in amorphous SiC [14]. *Ab initio* calculations using different computational techniques were used to study magnetic properties of SiC DMS theoretically. The results, again, were somewhat contradictory. While Cr and Mn were found to be ferromagnetic at the Si sites with different values of magnetic moment and magnetic coupling strength, Fe was found nonmagnetic in some cases and magnetic in others [15–20]. No spin polarization was reported for Co- and Ni-doped SiC [15, 16]. The results of the calculations were also found to be sensitive to the particular calculation technique employed. Little is known about the microscopic structure of the TM impurities in the SiC host, as well as about the details of lattice reconstruction and related effects.

In a recent communication [21] we reported that Fe in an SiC host can exist in both magnetic and nonmagnetic states which sensitively depend on the TM atom environment in the host matrix. The states were found to be separated by an energy gap comparable to the thermal energy at room temperature. Transition from one state to the other was accompanied by a significant reconstruction of the crystal lattice around the TM impurity. We argued that similar effects may be essential to other DMS systems and suggested a new approach to the problem of magnetic impurities in semiconductors, accounting for these multiple TM impurity states.

Here, we present the results of a systematic study of magnetic states of first row transition metal impurities in an SiC host, which were obtained using a highly accurate *ab initio* FLAPW calculation technique. We analyse the details of magnetic moments' formation and of their change with unit cell volume, as well as of the host lattice reconstruction due to impurity substitution. We also study the particulars of exchange interactions for different TM impurities and provide estimates of the magnetic ordering temperatures of SiC DMS.

2. Methodology and computational details

Electronic and magnetic properties of substitutional transition metal impurities in SiC are studied using the cubic 3C-SiC polytype as a model SiC DMS material system. All SiC polytypes share a hexagonal close-packed crystal lattice differing in the stacking sequences of the silicon–carbon bilayers. Here, we mostly focus on the magnetic moments' formation and their interaction, which is expected to be qualitatively independent of the long-range order and, therefore, the particular polytype the TM impurity substitutes in. Many common features peculiar to the electronic properties of different SiC polytypes have been revealed in prior studies [17, 18]. Certain quantitative differences are, however, expected to be caused by, for instance, the presence of different inequivalent lattice sites in the SiC lattice. While in all SiC polytypes the nearest neighbours of any Si or C atom are always four C or Si atoms, respectively, which form tetrahedra around the corresponding Si or C atom, there are two types of sites in the SiC lattice, different in their next-nearest-neighbour arrangement or the medium-range order. These are the so-called cubic and hexagonal sites or layers with the stacking sequences ABC and ABA, respectively [9]. There are only cubic layers in 3C-SiC, while other common polytypes such as 4H and 6H contain different numbers of both hexagonal and cubic layers. Although the electronic properties of an atom are expected to be influenced most strongly by its nearest neighbours, the type of the site the atom occupies, and thus its more distant neighbours, may also be important, as we will see below from the comparison of the properties of TM atoms in 3C-and 4H-SiC.

In the calculations we employ the cluster approach to model the lattice of single-crystal SiC with transition metal impurity. Cubic SiC possesses a zinc blende crystal lattice with the primitive cell consisting of one silicon–carbon pair. Another way of representing this type of lattice is with a sequence of hexagonal close-packed silicon–carbon bilayers with the ABC stacking sequence [9]. In the latter case the unit cell consists of three Si–C bilayers or six atoms. In calculations of electronic properties of pure and TM-doped SiC, as well as of magnetic moments of TM impurities in the SiC host, we used a supercell with a total of 18 atoms in three Si–C bilayers. The supercell used to calculate the properties of 4H-SiC, with which we compare our results, contains one more Si–C bilayer and thus consists of 24 atoms. Impurity atoms were placed in the centres of the adjacent close-packed hexagons, so that the distances between them both in-plane and in the z-axis direction were approximately equal, providing a uniform TM doping. Substitution of one atom per 3C-SiC supercell is equivalent to a TM doping concentration of about 5 at.%. Such concentrations are typical for experiments, including SiC DMS systems. The supercell we constructed places TM atoms in the Si sublattice. It now seems to be well established that the Si sublattice of the SiC lattice is more favourable for TM substitution [15, 16] and, therefore, we do not study substitution sublattice preference. The Si_8C_9TM lattice used in the calculations is presented in figure 1.

It has been shown in several earlier studies [18, 21] that electronic and magnetic properties of diluted magnetic semiconductors are influenced significantly by the lattice relaxation. In fact, letting the lattice relax after the impurity substitution may result in a completely different magnetic state of the TM impurities. In this study, prior to calculating any material properties, we perform a full inhomogeneous

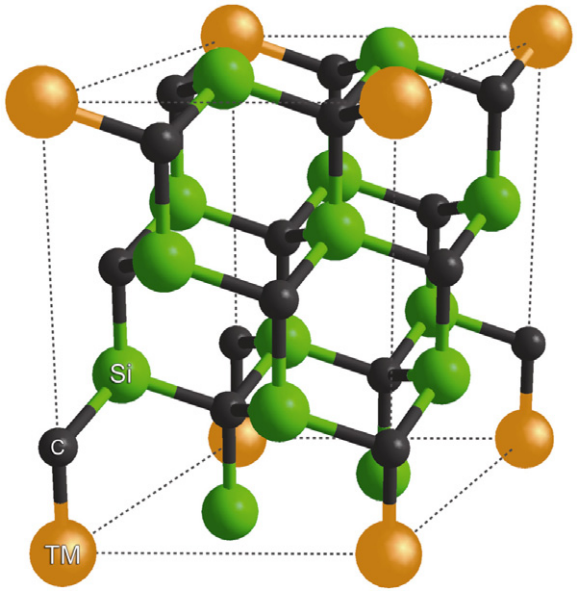

Figure 1. 3C-SiC-TM superlattice used in the calculations.

relaxation of the supercell by minimizing intra-cell forces and optimizing atomic positions for a number of volume values of the isotropically expanded lattice. We then fit the universal equation of state [22] to the calculated total energy-lattice volume dependences and find an optimal equilibrium volume of the unit cell. Electronic and magnetic properties of SiC DMS are then calculated for the supercell volume and the atomic positions corresponding to this equilibrium lattice geometry.

This study only includes neutral substitutional transition metal atoms in the SiC matrix. TM impurity concentrations of several atomic per cent discussed here are typical for DMS but very high compared to those used in electronic devices. This means that the position of the Fermi level and thus the charge states of all impurities in such a system are determined by the TM impurity. Changing the TM impurity charge state independently would require co-doping with a comparable amount of another donor or acceptor. On the other hand, reducing TM concentration to the typical heavy doping levels of, say, 10^{19} cm^{-3} would result in a 'very diluted semiconductor', where an efficient exchange interaction would be hindered by large distances between the transition metal atoms; we do not consider this latter case here. On the other hand, recently calculated formation energies of different charge states of TM impurities in SiC [16, 18] in their typical DMS concentrations indicate that all impurities under study here are expected to be in their neutral charge states.

Electronic structure and magnetic properties of 3C-SiC were calculated using the self-consistent full-potential linearized augmented plane wave (FLAPW) technique implemented in the EXCITING software package [23, 24]. Exchange–correlation potential was calculated using the generalized gradient approximation (GGA) according to the Perdew–Burke–Ernzerhof model [25]. Since we needed to resolve magnetic and nonmagnetic solutions close in energy, the accuracy of the calculations needed to be higher than at least the differences in energy between these solutions. To satisfy this requirement the following parameters were chosen for the calculations. The atomic radii were set to 2.0 au for Si and TM atoms and 1.5 au for carbon atoms. The APW basis set included 120 plane waves per atom. Within the atomic spheres, spherical harmonic expansions with angular momentum up to 8 were used for the wavefunction, charge density and potential representation. Local orbitals were added to the APW basis set to improve convergence and accuracy of the calculations. The self-consistent calculations were performed for 12 reciprocal lattice points in the irreducible wedge of the Brillouin zone and were considered converged when the RMS change in the effective potential was less than 10^{-6} and the total crystal energy error was within 1 meV/atom. To check our computational set-up, we calculated the equilibrium unit cell volume of pure 3C-SiC by finding the minimum of the crystal total energy as a function of the volume of the relaxed supercell. The calculated unit cell volume was found to be equal to 70.19 au^3/atom, which is in excellent agreement with the experimental value of 69.98 au^3/atom [9].

3. Magnetic moments

TM atoms in the SiC lattice experience different degrees of coupling with the host atoms, depending on the substitution atom's electronic structure and on the electronic configuration of the surrounding dangling bonds and more distant atoms in the lattice. In turn, substitution of a host atom by a TM atom results in SiC lattice reconstruction, which self-consistently defines the electronic and magnetic configuration of the DMS material. As has been shown in [21] for 4H-SiC, different DMS states, characterized by the corresponding lattice geometry, electronic density distribution (and thus chemical bond structure) and the corresponding different values of TM magnetic moments, may be realized. A similar behaviour is characteristic for some transition metals and alloys [26–28]. Different magnetic states of transition metal atoms in the SiC host may be realized (if not under equilibrium conditions) by either changing the lattice geometry in, for example, the lattice expanded due to ion implantation, or by making the magnetic state favourable by, for example, applying a magnetic field under high temperature equilibrium growth conditions. In the latter case, the magnetic state of the TM atoms leads to the corresponding lattice reconstruction, while rapid lattice cooling to the point where the atom mobility is low 'freezes' the magnetic state. Of course, the magnetic state, if energetically favourable, can also be realized in equilibrium conditions.

We found that all of the impurities studied may be present in the states with different values of the magnetic moment depending, in particular, on the lattice cell geometry. Figure 2 presents total energy volume curves for Fe-, Mn- and Co-doped 3C-SiC. These three impurities represent typical scenarios of magnetic state formation in SiC DMS. Obtained magnetic properties of Cr in 3C-SiC are qualitatively similar to those of Mn with a different total energy gap between nonmagnetic and magnetic solutions and different magnetic moment values, while Ni behaves similarly to

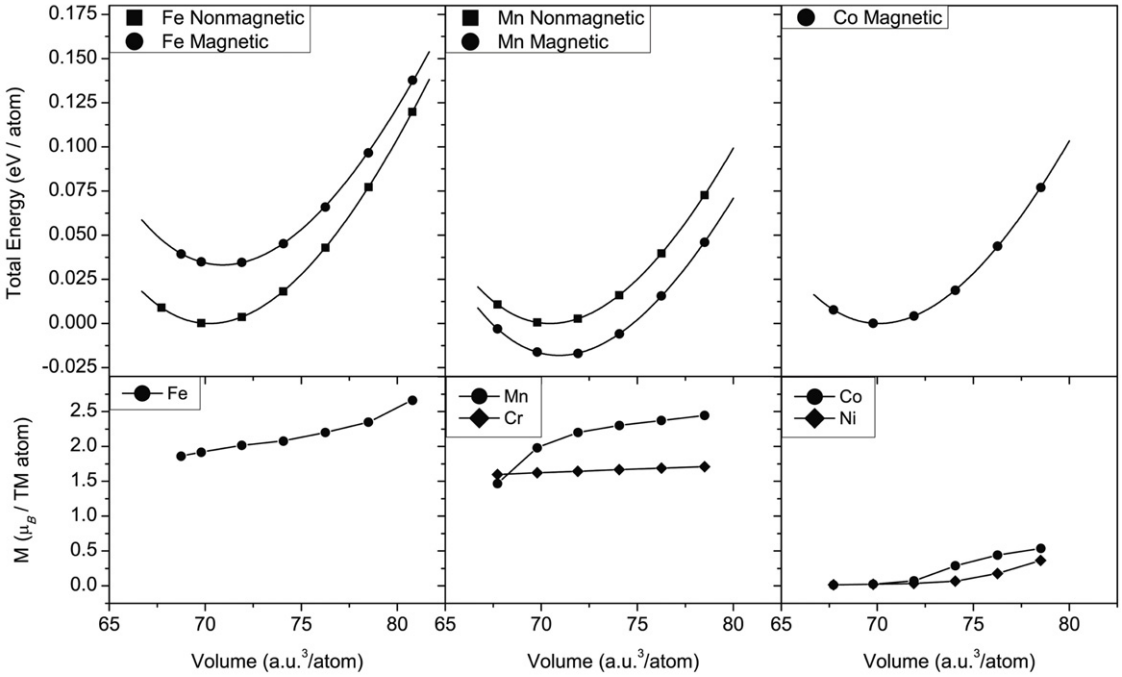

Figure 2. Energy–volume and magnetic moment–volume dependences for TM-doped 3C-SiC. At zero temperature, in Fe-doped SiC the magnetic solution is energetically unfavourable, while in SiC–Mn it is energetically favourable (the latter is also the case for SiC–Cr). For SiC–Co and SiC–Ni, the two solutions practically overlap in the range of the plot with the magnetic moment being quenched at lower (equilibrium) values of the cell volume.

Co. Unit cell volume or 'atomic volume' dependences of the total energy are multiple-valued for Fe, Mn and Cr at their corresponding equilibrium lattice volumes, representing magnetic and nonmagnetic states of TM atoms with different relationships between the two. Magnetic and nonmagnetic solutions practically coincide for Ni and Co, which is an expected result as the magnetic moment values of Ni and Co atoms in their magnetic states are rather small. Bottom panels of figure 2 present the corresponding values of the TM atomic magnetic moments.

It is important to keep in mind that the calculated total energy is a zero-temperature ground state quantity. At a nonzero temperature, the free energy entropy term will contain contributions due to both atomic position fluctuations of host and impurity atoms and, in the magnetic case, due to magnetic moment fluctuations (magnitude and direction). Per atom values of the two entropy terms should be of about the same order of magnitude, as similar thermal disordering processes create the corresponding microscopic configuration sets. An estimate of the atomic disorder entropy term [21] shows that it can be comparable to the energy gap between the nonmagnetic and magnetic states and may therefore change their relationship at a high enough temperature.

We also note here that the solutions described are obtained in a supercell containing a single TM impurity. This supercell is periodically replicated (implicitly) to form the SiC-TM crystal lattice. Therefore, by model lattice construction the TM impurities make up a periodic superlattice, while atomic spins, if they exist, are assumed to be aligned in parallel. In section 4 we provide the results of calculations for a supercell with two Si atoms substituted by TM atoms, which allows us to clarify whether the magnetic solutions obtained are either antiferromagnetic or, indeed, ferromagnetic. At the same time, in real systems periodicity may break due to configuration disorder. The disorder, depending on its degree, may affect both the magnetic moments and their ordering, and will require other computational techniques such as, for example, Monte Carlo methods for handling its effects. Our results reveal the general tendencies of magnetic moments' formation and interaction in SiC DMS and are expected to be a basis for the research taking more complicated issues, such as fluctuations and disorder, into account.

3.1. Fe-doped SiC

For iron-doped 3C-SiC, the magnetic state possesses larger energy with the energy difference between this and the nonmagnetic state of approximately 33 meV/atom. The magnetic state is realized in an expanded lattice with the volume per atom of approximately 70.90 au^3, which is 1% larger than the equilibrium average atomic volume in the lattice of pure 3C-SiC. Different atoms in the lattice shift differently as a result of the impurity substitution, with the tetrahedron of four C atoms around the Fe atom being affected most strongly. The expansion of this tetrahedron was found to be as large as 10 vol%. The equilibrium lattice volume of 70.23 au^3/atom for 3C-SiC–Fe in the nonmagnetic state is practically equal to that of pure 3C-SiC, while the atomic position changes were found to be minimal. It is worth mentioning that the magnetic solution in Fe–SiC DMS was not obtained as a result of a fixed spin moment calculation. Rather, the calculations naturally converge to the magnetic solution when started from

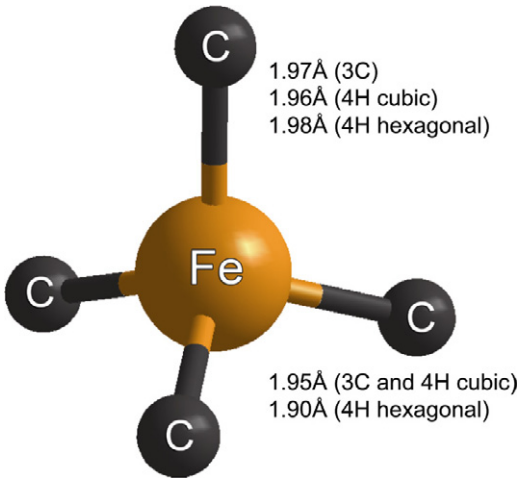

Figure 3. Details of C bond relaxation around the Fe atom needed to achieve high-spin state in different SiC polytypes and inequivalent lattice sites. Fe–C bond lengths for nonmagnetic Fe and Si–C bond lengths in undoped SiC are approximately equal to 1.89 Å.

a sufficiently expanded lattice. The entire $E(V)$ curve is then obtained by using the solution at each point as an initial approximation for the next one.

The energy gap between the magnetic and nonmagnetic solutions of approximately 33 meV/atom in 3C-SiC–Fe is different from the value of 20 meV/atom we found in our earlier study for 4H-SiC [21]. The nature of the atomic relaxation in the two polytypes is also rather different. In 4H-SiC, the relaxation due to the substitution of magnetic Fe atoms strongly affected the carbon atom above the Fe atom in the z direction while the other three atoms in the tetrahedron shifted noticeably less (cf figure 1). In 3C-SiC the relaxation is nearly equilateral so that the elemental tetrahedra around Fe atoms expanded evenly. As already mentioned, in 3C-SiC the stacking sequence is such that all lattice sites are equivalent and have cubic symmetry. In 4H-SiC there are sites with different, hexagonal and cubic, symmetries, and in our previous study [21] Fe substituted on the hexagonal site. In the present work, for comparison with 3C-SiC, we studied 4H-SiC with the magnetic Fe substituting on the cubic site. We found that in this case lattice relaxation is similar to that in 3C-SiC, with the C tetrahedra around Fe atoms expanding equilaterally. The details of the lattice relaxation, including the distances the other atoms in the supercell shift, are, however, different in all three cases studied. We can thus confirm that the SiC-TM lattice structure, and therefore electronic and magnetic properties of substitution TM atoms, depend not only on their closest environment but also noticeably on the long-range stacking sequence. Figure 3 presents the particulars of the elemental tetrahedron bond length relaxation in different SiC polytypes and inequivalent lattice sites.

The magnetic moment of Fe in 3C-SiC changes approximately linearly from about 1.9 to 2.6 μ_B/Fe in the range of volumes that we performed the calculations for. The fact that the magnetic and nonmagnetic solutions are so close on the energy scale allowed us to suggest [21] that, at high enough temperature, a new equilibrium mixed state with a certain distribution of TM atoms between the two states may be realized, with the total value of the magnetic moment being equal to an average over the two states. Such state mixing may, together with other factors, explain the smaller, compared to calculated, values of the experimentally observed magnetic moments reported for, for instance, GaN-based DMS materials [29–31].

3.2. Mn- and Cr-doped SiC

Manganese and chromium represent another kind of behaviour of TM in a 3C-SiC host. In Mn- and Cr-doped SiC the relationship between the nonmagnetic and magnetic solutions is the opposite of that in SiC–Fe, with the magnetic solution being more energetically favourable. The magnetic state is more 'stable' in Cr-doped 3C-SiC, with the total energy difference between the solutions of approximately 45 meV/atom compared to less than 20 meV/atom in SiC–Mn. At a nonzero temperature, if the magnetic–nonmagnetic state mixing takes place, the average magnetic moment in SiC–Mn may be expected to go down more significantly than in SiC–Cr. Volume dependences of the atomic magnetic moments are very different for Mn- and Cr-doped SiC. While the magnetic moment of Cr atoms changes only slightly from 1.6 to 1.7 μ_B in the range of average atomic volumes from 68 to 76 au^3/atom, the magnetic moment of Mn experiences a steep increase from 1.5 μ_B at 68 au^3/atom and then almost saturates at approximately 2.5 μ_B for larger values of the atomic volume. Such behaviour of atomic magnetic moments can be related to the larger stability of the Cr magnetic state caused by the fact that the electronic structure of substitutional Cr is less dependent, compared to that of Mn, on the host lattice environment (see the discussion below). The values of magnetic moment at equilibrium volume of about 1.65 μ_B and 2.1 μ_B per atom for Cr and Mn, respectively, are close to those found by Shaposhnikov and Sobolev [17].

The character of atomic relaxation is completely different for SiC–Mn and SiC–Cr. In magnetic SiC–Cr the optimal lattice volume is equal to 71.10 au^3/atom, which is an approximately 1.3% change compared to pure 3C-SiC. This expansion is again, as in the case of Fe, absorbed mostly by the reconstruction of the tetrahedron around the Cr atom. The relative (compared to pure SiC with the same unit cell volume) change of the volume of this tetrahedron is close to 6% and the relaxation is isotropic. The lattice geometry is practically independent of the volume, i.e. no additional reconstruction happens as the lattice is expanded or shrunk. Interestingly, in contrast to SiC–Fe, there is also a noticeable lattice relaxation in the case of substitutional Cr in the nonmagnetic state with the average atomic volume change of about 0.8% and the Cr neighbouring tetrahedron expansion of about 4 vol%. In magnetic SiC–Mn, the equilibrium lattice volume is 1% larger than in pure 3C-SiC, while the tetrahedron around Mn atoms expands by approximately 4% at equilibrium volume. Some noticeable relaxation is experienced by Si atoms in the layers other than the layer where the TM substitutes. As the crystal lattice is expanded from its equilibrium volume, the tetrahedron expands further, and at

the lattice volume of 76 au^3/atom its relative volume becomes 6% larger than in the undoped crystal. The average atomic volume of 70.47 au^3/atom of 3C-SiC–Mn in the nonmagnetic configuration is very close to that of pure SiC.

The described differences in the lattice structure and reconstruction in SiC doped with different TM impurities are related to their different magnetic behaviours. The different magnetic states and their changes with atomic volume are dependent (self-consistently) on the structure of the TM electronic orbitals. In a tetrahedral environment, TM d states split into t_2 and e symmetry combinations. Electron density corresponding to e state wavefunctions is concentrated along x, y and z directions, whereas for t_2-type wavefunctions it is concentrated along the diagonals, approximately in the directions of the neighbouring C dangling bonds. The latter also form t_2 symmetry states with energies close to those of TM t_2 states and can couple with them forming bonding and anti-bonding states. Following the discussion of Miao and Lambrecht [18], we note that Cr d electrons fill nonbonding e states, while Cr t_2 states are empty, and thus the coupling of Cr d states to the surrounding C states is weak and the d states are rather localized. Therefore Cr atoms are expected to experience a smaller influence of the host crystal environment and the volume dependence of their electronic and magnetic properties is smaller. Mn has one more electron, which starts to occupy the anti-bonding t_2 states. The latter couple stronger to the surrounding atoms' orbitals and are thus more delocalized. This stronger coupling results in a stronger, compared to Cr, dependence of Mn electronic properties on its environment.

3.3. Ni- and Co-doped SiC

Nickel and cobalt represent the third type of behaviour of transition metals in a 3C-SiC matrix. We found that for both Ni and Co the magnetic and nonmagnetic solutions for their crystal total energy volume dependences are very close (for instance, in the range of the plot of figure 2 the difference for SiC–Co is negligible at equilibrium volume and about 2 meV/atom at the volume of 78 au^3/atom). The equilibrium cell volumes of 70.4 au^3/atom in the case of Ni and 70.07 au^3/atom in the case of Co are practically equal to that of pure 3C-SiC. The latter value is even a little smaller than the average atomic volume in the pure material, so that Co substitution leads to a slight host lattice contraction. Both SiC–Co and SiC–Ni are practically nonmagnetic in their equilibrium configurations, with the magnetic moments of about 0.02 μ_B/TM atom. The magnetic moments go up noticeably as the SiC-TM lattice is expanded, reaching almost 0.4 μ_B/Ni and 0.5 μ_B/Co at the average atomic volume of 78 au^3/atom. Remarkably, although for SiC–Ni and SiC–Co the average equilibrium atomic volume experiences practically no change compared to pure SiC, the 3C-SiC lattice reconstruction due to Ni and Co substitution turns out to be rather strong. The expansion of the tetrahedra around the substitution atoms reaches 3% for SiC–Co and is as large as 10% in SiC–Ni at their optimal cell volumes. This local relaxation is compensated by the corresponding changes in other, primarily Si, atom positions so that the average per atom lattice volume remains almost equal to that in pure 3C-SiC. As the lattice of SiC–Ni or SiC–Co is expanded, accompanied by the magnetic moment growth, the tetrahedra containing the TM atoms expand even further, with their relative (to pure SiC with the same unit cell volume) volumes reaching 13% for Ni and 4% for Co at the average volume value of 78 au^3/atom. At the same time, relaxation of the rest of the supercell reduces with the Si atoms returning to the positions characteristic of pure material, indicating that these atoms provide the supercell rigidity preventing the TM-C tetrahedra from expanding further and the TM atoms from possibly reaching the high-spin state. Another noteworthy fact is that, in the case of Co and Ni substitution, the transition from practically nonmagnetic to magnetic state and the corresponding lattice reconstruction occur gradually, while in Mn-, Cr-and Fe-doped SiC the two states are separated by a significant potential step/barrier. It is also interesting that, in all cases presented in figure 2, the TM atomic magnetic moments increase with atomic volume. One can therefore rather simplistically state that the TM atom 'needs' more space for itself in the host lattice to acquire a magnetic moment. Such a picture may be useful for visualization of the described relaxation processes characteristic for the magnetic and nonmagnetic states of the TM impurities. Table 1 summarizes the properties of different magnetic states of the TM impurities in 3C-SiC DMS. In addition to the quantities already discussed, the table includes the average magnitude of the magnetic moments at room temperature estimated assuming that the energy relationship between the magnetic and nonmagnetic states remains the same as at zero temperature and using the Boltzmann distribution function for calculation of the occupation probabilities.

4. Magnetic ordering

The calculations of magnetic moments presented in the previous section were done for a supercell with a single TM impurity. In the crystal constructed in such a way, the magnetic moments of the impurities order in parallel due to periodicity. In this section we study how an introduction of a pair of TM impurities into the SiC lattice changes the spin ordering. We constrain ourselves to only Cr-, Mn-and Fe-doped 3C-SiC, as the magnetic moments of Co and Ni are practically zero at the equilibrium cell volume and are also rather small even in an expanded lattice. We study the magnetic ordering for two different spatial configurations of TM impurities in the SiC lattice. First, we simply double the supercell shown in figure 1 in the z direction so that there are two TM atoms per supercell at a distance of 14.27 au, while their concentration is kept at 5 at.%. Next, we return to the original Si_8C_9TM supercell and introduce an additional TM atom as the nearest neighbour to the TM atom in the Si-TM plane (cf figure 1). The distance between the TM impurities in this case equals 5.82 au and their effective concentration is approximately 10%. We then calculate the total energies of both types of supercells with TM spins ordered in parallel and anti-parallel. The energy difference ΔE_{FM-AFM} between the FM and AFM configurations reveals the strength of the exchange coupling

Table 1. Properties of TM-doped 3C-SiC: energy differences between ferromagnetic and nonmagnetic states, $\Delta E_{\mathrm{FM-NM}}$; magnetic moments at equilibrium cell volume, M_0, and at the cell volume of 78 au^3/atom, M_1; the average over the two states' magnetic moment at room temperature and equilibrium cell volume, M_A; equilibrium unit cell volume change, ΔV_0, and change of the volume of the tetrahedra around impurity atoms, ΔV_T, relative to pure SiC. Note that, for Co and Ni, ΔV_T corresponding to the magnetic state is given at the cell volume of 78 au^3/atom, while for the other impurities it is given for the magnetic state equilibrium cell volume.

TM species	$\Delta E_{\mathrm{FM-NM}}$ (meV/atom)	M_0 (μ_B/TM)	M_1 (μ_B/TM)	M_A (μ_B/TM)	ΔV_0 (%) NM/FM	ΔV_T (%) NM/FM
Cr	−46	1.63	1.71	1.40	0.8/1.3	4.4/6.3
Mn	−18	2.09	2.44	1.40	0.4/1.1	1.6/4.4
Fe	33	1.92	2.35	0.42	0.1/1.0	0.3/10
Co	0	0.03	0.53	0.03	−0.2	3.2/4.4
Ni	0	0.02	0.36	0.02	0.3	9.8/13

Table 2. Energy differences between ferromagnetic and antiferromagnetic configurations and mean-field values of the Curie temperature for TM-doped 3C-SiC with different distances between the TM impurities d_{TM}. The negative Curie temperatures can be interpreted as the positive Néel temperatures.

	$\Delta E_{\mathrm{FM-AFM}}$ (meV/cell)		Mean-field T_C (K)	
TM species	$d_{\mathrm{TM}} = 14.27$ au	$d_{\mathrm{TM}} = 5.82$ au	$d_{\mathrm{TM}} = 14.27$ au	$d_{\mathrm{TM}} = 5.82$ au
Cr	5	−222	−19	859
Mn	−56	−70	216	270
Fe	107	221	−412	−854

between the TM impurities. Using this energy difference, we provide a rough estimate of the Curie temperature using the mean-field expression:

$$T_C = -\frac{1}{3k_B}\Delta E_{\mathrm{FM-AFM}},$$

where k_B is the Boltzmann constant.

4.1. Magnetic coupling strength and range

SiC-TM FM–AFM energy differences and the corresponding Curie temperatures are summarized in table 2. Calculations show that both the strength and range of the exchange interaction differ significantly for Cr, Mn and Fe substituting in a 3C-SiC host lattice. In the nearest-neighbour arrangement, the ferromagnetic order of Cr and the antiferromagnetic order of Fe atoms are very stable with the absolute values of the FM–AFM energy difference of about 220 meV and the corresponding high ordering temperatures. The coupling strength reduces, although still being significant when Fe atoms are drawn further apart, while their magnetic moment alignment remains antiferromagnetic. At the same time, the interaction between Cr atoms reduces drastically when they are spaced by two Si–C bilayers, dropping to an almost negligible value of 5 meV. Although there is also a change of sign of the exchange coupling of Cr atoms in this configuration, we do not attach any physical meaning to this fact as such small absolute values of the total energy are comparable to the accuracy of our calculations. As mentioned above, the electrons in the Cr impurity in the SiC host fill the strongly localized e state, while Cr nonbonding t_2 states are empty. This explains the short-ranged nature of the magnetic coupling between Cr atoms. Fast decay of the magnetic coupling between the Cr atoms was also reported by Miao and Lambrecht as a result of their FP-LMTO calculations [18]. The authors found a similar behaviour for the Cr impurity in both 3C- and 4H-SiC with the FM–AFM energy differences close to our values. Kim *et al* recently studied the properties of Cr in 3C-SiC by the ultrasoft pseudopotential method [19]. Their results are different from ours with much larger FM–AFM energy differences which increase at intermediate Cr concentrations of 6–12% and then drop at the very high concentration of 25%. In principle, a full-potential LAPW basis should be more reliable compared to the pseudopotentials in describing the subtle effects of atomic orbital hybridization, structural relaxation and itinerant behaviour which, as has been mentioned above, are important for the correct treatment of magnetism in the DMS systems.

Substitutional Mn is ferromagnetic in 3C-SiC and exhibits a different ordering behaviour with the strength of magnetic coupling several times smaller compared to Fe and Cr and reaching the value of 70 meV for the nearest-neighbour pair. For larger Mn–Mn distances the magnetic interaction reduces only slightly. Such behaviour can again be explained by the nature of the partially filled Mn anti-bonding t_2 states, which due to their symmetry couple more with the surrounding atoms and are therefore more delocalized. Our values of the Mn coupling energy for the nearest neighbours are larger than those reported by Miao and Lambrecht [18] (70 meV versus ∼20 meV) and also show a somewhat different behaviour with regard to the Mn atom separation. At an Mn–Mn distance of ∼14 au, the magnetic coupling calculated in [18] changes the sign and becomes antiferromagnetic, while our calculations show almost no change compared to the nearest-neighbour case with the corresponding relatively large value of the ordering temperature. Besides the difference in the computational method used to produce these results, for approximately the same (∼14 au) Mn–Mn distance the authors of [18] may have chosen a different Mn substitution site in the SiC lattice. In general, exchange interaction between the TM impurities may further depend on their orientation and

be influenced by other impurity atoms in the same supercell and further away in the lattice. These aspects will need an additional study. It is also important to keep in mind that the mean-field calculations usually overestimate the Curie temperature values for low impurity concentrations, especially for the short-range exchange interaction. The problem is with securing a percolation of ferromagnetic ordering throughout the entire sample. In the case of longer-range exchange interaction the difference between the mean-field results and those obtained by, for example, a more sophisticated Monte Carlo method becomes smaller.

Analysing tables 1 and 2 one may conclude that the energy differences between the ferromagnetic and antiferromagnetic states are larger than the energy differences between the ferromagnetic and nonmagnetic states for all impurities. However, these two quantities are normalized in different ways and therefore cannot be compared directly. The first quantity is the total energy difference between the FM- and AFM-ordered supercells containing a pair of TM atoms, and is the amount of energy needed to flip the spin of one of these atoms, thus describing the strength of their magnetic ordering (which is used in the corresponding mean-field Curie temperature expression). The second quantity is the average *per atom* amount of total energy needed to reconstruct the crystalline lattice in such a way that the TM atom in this lattice acquires or loses its magnetic moment. If both the FM–AFM and FM–nonmagnetic energy differences are normalized similarly (per atom or per supercell), the first difference becomes in all cases smaller than the second, indicating that the FM–AFM energy difference can be thought of as an additional 'small splitting' of the corresponding magnetic state. Therefore, while for example the antiferromagnetic state of Fe atoms is more favourable compared to the ferromagnetic state, it is still significantly higher in energy compared to the nonmagnetic state (the energy difference is $\sim$3 meV/atom between FM and AFM states and 33 meV/atom between FM and nonmagnetic states for 5% Fe concentration). This makes the nonmagnetic state the ground state in SiC–Fe.

Because of the self-consistent relationship between the DMS structure and TM magnetic moment values and directions, the ferromagnetic and antiferromagnetic states of the DMS are characterized not only by the different values of the total energy but also by different atomic and electronic structures and, consequently, different magnetic moments. The differences between the FM and AFM states depend on the nature of TM electronic orbitals. While the change of bond length relaxation between the two states was found to be relatively small compared to the corresponding changes between the (ferro)magnetic and the nonmagnetic states, there is a certain difference in the values of the magnetic moments, which is negligible for Cr, reflecting the very localized nature of Cr atoms' electronic density, and reaching a 20% reduction for Mn atoms in the antiferromagnetic state compared to their ferromagnetic state. Again, since these calculated properties correspond to the ground state of the DMS, an additional study is needed to reveal the corresponding relationships for a nonzero temperature condition, where all three, FM, AFM and nonmagnetic, states may mix, creating a new state of the DMS.

4.2. Densities of states and the nature of exchange interaction in SiC-TM

Understanding the nature of exchange coupling in DMS is an important problem in magnetic materials. As has been pointed out by Belhadji *et al* [32], certain characteristic features of the DMS densities of states are important in identification of the exchange mechanisms responsible for magnetic coupling as well as in predicting the coupling strength and range. We calculated partial densities of states of Cr, Mn and Fe in 3C-SiC. They are presented in figure 4. In Cr-doped SiC the Fermi level falls between the majority e and anti-bonding t_2 bands, the former being fully filled and the latter being empty. Hybridization between the e and t_2 states of the majority spin channel results in the filled e states shifting to lower energies. The resulting energy gain stabilizes ferromagnetism by superexchange. This energy gain scales linearly with the impurity concentration and is proportional to the square of the hopping matrix element between the e and t_2 states, which is relatively small due to the localized nature of the e orbitals. Additionally, the strength of magnetic interaction is expected to fall off quickly with the TM–TM distance and the corresponding ordering temperature is strongly dependent on TM concentration.

One more electron per TM in SiC–Mn is in the majority channel anti-bonding t_2 state and the Fermi level falls within the t_2 band. In this situation, the energy is gained by aligning Mn spins in parallel, which then leads to broadening of this band and shifting of the weight of the electron distribution to lower energies. This is Zener's double-exchange mechanism which also leads to ferromagnetism [33, 34]. The impurity bandwidth and thus the energy gain due to double exchange scales as the square root of impurity concentration and is linear in the hopping matrix element between the neighbouring impurities. This square root dependence implies relatively large values of T_C already at small impurity concentrations if, at the same time, the interaction range is large enough for exchange to percolate through the crystal. The ferromagnetic superexchange interaction due to coupling between the majority e and almost empty t_2 states, although weaker than in SiC–Cr because of the larger energy difference between these states, provides an additional stabilization of the ferromagnetic state in SiC–Mn.

An additional mechanism, which is characteristic of this band structure and acts in competition with the double exchange, is the antiferromagnetic superexchange [32]. The wavefunctions of the majority e and t_2 states hybridize with the antiferromagnetically aligned e and t_2 states of the opposite spin channel. As a result, the lower in energy states are shifted to even lower energies and the higher states are shifted to higher energies. The energy is gained by reduction of the energy of filled states. The mechanisms of ferromagnetic and antiferromagnetic superexchange interactions are similar; whether the parallel or the anti-parallel alignment will be more energetically favourable depends on the strength of hybridization of states in the same and in the opposite spin channels. The double-exchange-stabilized ferromagnetic state is more favourable if the Fermi level lies well within the impurity band, while the energy gain due to superexchange

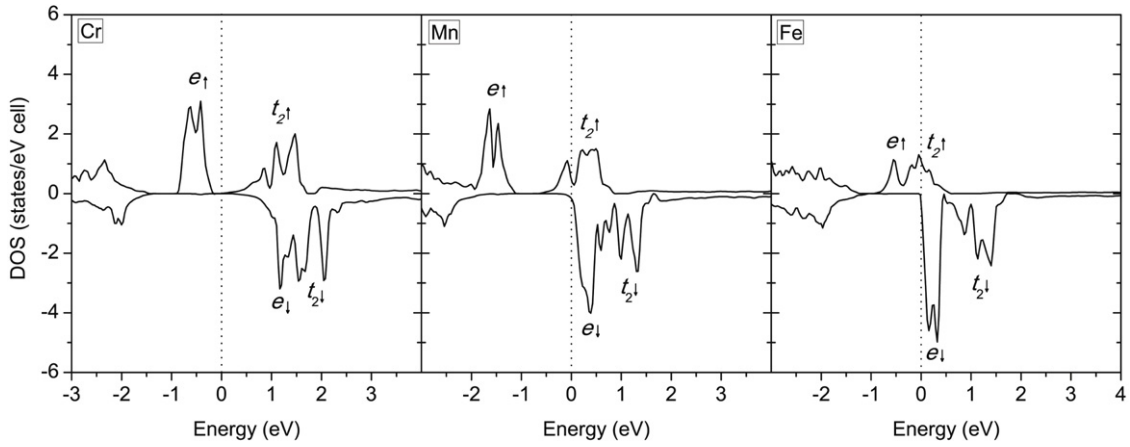

Figure 4. Partial densities of states of TM impurities in 3C-SiC. Origin of the energy axis corresponds to the Fermi level position.

is larger when the Fermi level lies between the bands of the same or opposite spin channels or near the band edges [32]. In SiC–Mn the hybridization of the majority and minority e states is rather weak because of their localized nature and relatively large energy difference between the two. Hybridization between the t_2 states is stronger, but only a small fraction of these states is filled, so in SiC–Mn double exchange wins, stabilizing ferromagnetism.

In Fe-doped SiC, there is again a competition between the ferromagnetic double-exchange and the antiferromagnetic superexchange mechanisms. However in this case, the Fermi level is close to the top of the majority bands and separates the majority and minority bands. The energy gain due to double exchange is reduced because of the nearly complete filling of the anti-bonding majority t_2 band. At the same time, the superexchange becomes more favourable due to the stronger hybridization between the e and t_2 bands in different spin channels. This explains why the antiferromagnetic ordering is favoured in 3C SiC–Fe. It is also worth mentioning that the partial DOS of Fe in 3C-SiC is very similar to the DOS of Fe-doped 4H-SiC. Thus, antiferromagnetic ordering is expected to be inherent to 4H SiC–Fe DMS too.

Recalling that the calculations are performed for the ground state of the DMS, we note that only the direct exchange mechanisms can be accounted for in our model. At a nonzero temperature and if a sufficient concentration of free carriers is created in the DMS, carrier-mediated exchange can also be important. Depending on the concentrations of TM and other impurities and the details of the material atomic and electronic structure, different exchange channels may play different roles in stabilizing an ordered magnetic state. In particular, different free carrier and TM atom concentrations may result in RKKY-type exchange interactions of different signs and having an oscillating character depending on the distance between magnetic TM impurities. Contribution of this carrier-mediated exchange may favour ferromagnetic, antiferromagnetic or spin-glass-like order. The resulting effective magnetic ordering will depend on the relative strengths of the direct and carrier-mediated indirect exchange interactions.

4.3. Comparison to experimental data

Finally, we compare our results to available experimental data. In a recent communication [14], Jin *et al* reported 10% Cr-doped amorphous SiC to be ferromagnetic above room temperature with the average magnetic moment of 0.27 μ_B. Although a Cr concentration of 10% approximately corresponds to the $Si_7C_9Cr_2$ supercell for which we obtained a large value of the ordering temperature, it should be kept in mind that effectively this result was obtained for the nearest-neighbour dimers. As the magnetic interaction was found to drop off quickly beyond the nearest neighbours, for a random impurity distribution it would likely not percolate through the lattice. Although the authors reported their samples to exhibit hole conductivity, it was likely due to residual impurities in the material since, according to the calculations [18], both Cr donor and acceptor levels are deep in the gap and cannot be the source of free carriers. Nevertheless, the existence of free holes may have led to an additional, hole-mediated exchange interaction playing the role in stabilizing ferromagnetism at larger distances between the impurities.

At least some of the experimental studies of Fe-doped SiC reported ferromagnetic DMS behaviour in Fe-implanted 6H-SiC [10, 11]. Our calculations reveal antiferromagnetic ordering in Fe-doped 3C-SiC. Such a discrepancy may be explained by several factors. First, our calculations were done for the TM impurities in the SiC lattice distributed either homogeneously or in the nearest-neighbour pair configuration, the latter representing the simplest case of TM nanocluster. Various other substitution TM configurations are possible and, as has been shown by Cui *et al* [35] for GaN–Cr DMS, the different nanocluster complexes, including substitutional and interstitial TM atoms, not only may be more favourable for formation compared to the homogeneous or random impurity distributions, but also can significantly alter magnetic properties of the DMS such as ordering type and temperature. The various cluster configurations can coexist in a statistical distribution, further complicating the physical picture. The resulting material properties will then be very sensitive to the growth and processing conditions. The strong sensitivity of magnetic properties of SiC DMS to the details of lattice

geometry and reconstruction due to TM substitution which we found in this study also supports these observations. Contribution of secondary phases to the magnetic signal can also not be ruled out completely [11]. The ferromagnetic response with the Curie temperatures of 250 K in 5% Mn-implanted 6H-SiC reported in [10] matches our estimates most closely. Further experimental work is, however, needed to unambiguously determine the origins of the magnetic signal in SiC DMS doped with different TM impurities.

5. Concluding remarks

Using the highly accurate FLAPW calculations technique, we have established that all transition metal impurities studied can exist in both the magnetic and nonmagnetic states in a 3C-SiC host matrix. For Cr, Mn and Fe the magnetic state can be realized at an equilibrium lattice volume and is separated by an energy gap from the nonmagnetic state, while for Ni and Co magnetic moments are close to zero in the equilibrium lattice and increase while the lattice is expanded. At zero temperature, a magnetic solution is energetically favourable in Cr- and Mn-doped SiC, while for Fe-doping a nonmagnetic solution is favoured. The energy differences between ferromagnetic and nonmagnetic solutions vary from impurity to impurity, being comparable to thermal energy at room temperature for Mn and Fe, and somewhat larger for Cr. As in our earlier communication [21], we argue that at a nonzero temperature the relationship between the solutions can change due to the free energy entropy term. Furthermore, we speculate that a mix of the magnetic and nonmagnetic states is possible, which would change the average magnetic moment of the system and self-consistently the magnetic order. TM substitution leads to a significant host SiC lattice reconstruction in all cases except when Mn and Fe are in their nonmagnetic states, in which case the atomic positions are very close to those in pure SiC.

The values of magnetic moments, magnetic moment ordering strength and range vary significantly across the range of impurities studied. While magnetic moments of Ni and Co grow noticeably, starting from very small values at equilibrium unit cell volume, they are still rather small ($\sim$0.5 μ_B) even in a 4% expanded lattice. Even though the calculated lattice parameters correspond to zero temperature conditions, given the values of the thermal expansion coefficient of SiC [36], such expanded lattice volumes cannot be reached by thermal expansion at practical temperatures. Thus Ni- and Co-doped SiC is practically nonmagnetic and will probably not be suitable for spin injection or other spin-electronic applications. Cr, Mn and Fe can exist in high-spin states in an SiC matrix. We found that magnetic Fe in SiC orders antiferromagnetically, while Cr and Mn prefer ferromagnetic ordering. The magnetic interaction between Cr atoms was found to be strong but short-ranged, whereas Mn–Mn interaction, although weaker, was found to be almost independent of the interatomic distance. The resulting mean-field Curie temperature in the nearest-neighbour configuration was estimated to be 270 K for SiC–Mn and as high as 859 K for SiC–Cr and DMS, dropping to 216 K and to a negligible value of 5 K for the 5% concentration of Mn and Cr impurities, respectively.

Given the long-range character of Mn–Mn exchange interaction in an SiC host, among the impurities studied Mn is perhaps the most promising candidate for achieving room temperature DMS behaviour, particularly if free carriers are present to enhance the magnetic interaction. High values of the Curie temperature might be realized in SiC–Cr DMS if long-range carrier-mediated exchange is present. However, in contrast to the now classical GaAs–Mn DMS, TM impurity energy levels in SiC are all expected to be deep donors or acceptors [18], and introduction of free carriers into SiC DMS may require co-doping with a shallow group III or V impurity in addition to a TM. The shallow impurity doping concentration needs to be comparable to the TM concentration to produce a significant free carrier concentration. This entails a further reconstruction of the host lattice and is subject to the difficulties related to solubility limits. Reduction of TM concentration for keeping the total impurity concentration reasonable will significantly weaken direct exchange in the case of SiC–Cr while for SiC–Mn the change is expected to be not as large, giving the latter another advantage in achieving room temperature ferromagnetic behaviour.

References

[1] Gregg J F, Petej I, Jouguelet E and Dennis C 2002 *J. Phys. D: Appl. Phys.* **35** R121
[2] Žutić I, Fabian J and Sarma S D 2004 *Rev. Mod. Phys.* **76** 323
[3] Bratkovsky A M 2008 *Rep. Prog. Phys.* **71** 026502
[4] Olejník K, Owen M H S, Novák V, Mašek J, Irvine A C, Wunderlich J and Jungwirth T 2008 *Phys. Rev.* B **78** 054403
[5] Dietl T, Ohno H, Matsukura F, Cibert J and Ferrand D 2000 *Science* **287** 1019
[6] Dietl T, Ohno H and Matsukura F 2001 *Phys. Rev.* B **63** 195205
[7] Pearton S J, Abernathy C R, Overberg M E, Thaler G T, Norton D P, Theodoropoulou N, Hebard A F, Park Y D, Ren F, Kim J and Boatner L A 2003 *J. Appl. Phys.* **93** 1
[8] Hebard A F, Rairigh R P, Kelly J G, Pearton S J, Abernathy C R, Chu S N G and Wilson R G 2004 *J. Phys. D: Appl. Phys.* **37** 511
[9] Bechstedt F, Käckell P P, Zywietz A, Karch K, Adolph B, Tenelsen K and Furthmüller J 1997 *Phys. Status Solidi* b **202** 35
[10] Theodoropoulou N, Hebard A F, Chu S N G, Overberg M E, Abernathy C R, Pearton S J, Wilson R G, Zavada J M and Park Y D 2002 *J. Vac. Sci. Technol.* A **20** 579
[11] Stromberg F, Keune W, Chen X, Bedanta S, Reuther H and Mücklich A 2006 *J. Phys.: Condens. Matter* **18** 9881
[12] Syväjärvi M, Stanciu V, Izadifard M, Chen W M, Buyanova I A, Svedlindh P and Yakimova R 2004 *Mater. Sci. Forum* **457–460** 747
[13] Huang Z and Chen Q 2007 *J. Magn. Magn. Mater.* **313** 111
[14] Jin C G, Wu X M, Zhuge L J, Sha Z D and Hong B 2008 *J. Phys. D: Appl. Phys.* **41** 035005
[15] Gubanov V A, Boekema C and Fong C Y 2001 *Appl. Phys. Lett.* **78** 216
[16] Miao M S and Lambrecht W R L 2003 *Phys. Rev.* B **68** 125204
[17] Shaposhnikov V L and Sobolev N A 2004 *J. Phys.: Condens. Matter* **16** 1761
[18] Miao M S and Lambrecht W R L 2006 *Phys. Rev.* B **74** 235218
[19] Kim Y S and Chung Y C 2005 *IEEE Trans. Magn.* **41** 2733
[20] Kim Y S, Chung Y C and Yi S C 2006 *Mater. Sci. Eng.* B **126** 194
[21] Los A V, Timoshevskii A N, Los V F and Kalkuta S A 2007 *Phys. Rev.* B **76** 165204

[22] Vinet P, Rose J H, Ferrante J and Smith J R 1989 *J. Phys.: Condens. Matter* **1** 1941
[23] Dewhurst J K, Sharma S and Ambrosch-Draxl C 2004 http://exciting.sourceforge.net
[24] Singh D J and Nordstrom L 2006 *Planewaves, Pseudopotentials, and the LAPW Method* 2nd edn (Berlin: Springer) ISBN 978-0-387-28780-5
[25] Perdew J P, Burke K and Ernzerhof M 1996 *Phys. Rev. Lett.* **77** 3865
[26] Moruzzi V L and Marcus P M 1988 *J. Appl. Phys.* **64** 5598
[27] Moruzzi V L, Marcus P M and Kubler J 1989 *Phys. Rev.* B **39** 6957
[28] Wassermann E F 1991 *J. Magn. Magn. Mater.* **100** 346
[29] Park S E, Lee H J, Cho Y C, Jeong S Y, Cho C R and Cho S 2002 *Appl. Phys. Lett.* **80** 4187
[30] Singh R K, Wu S Y, Liu H X, Gu L, Smith D J and Newman N 2005 *Appl. Phys. Lett.* **86** 012504
[31] Lee J S, Lim J D, Khim Z G, Park Y D, Pearton S J and Chu S N G 2003 *J. Appl. Phys.* **93** 4512
[32] Belhadji B, Bergqvist L, Zeller R, Dederichs P H, Sato K and Katayama-Yoshida H 2007 *J. Phys.: Condens. Matter* **19** 436227
[33] Sato K, Dederichs P H, Katayama-Yoshida H and Kudrnovský J 2004 *J. Phys.: Condens. Matter* **16** S5491
[34] Akai H 1998 *Phys. Rev. Lett.* **81** 3002
[35] Cui X Y, Medvedeva J E, Delley B, Freeman A J and Stampfl C 2007 *Phys. Rev.* B **75** 155205
[36] Taylor A and Jones R M 1960 *Silicon Carbide—a High Temperature Semiconductor* ed J R O'Connor and J Smiltens (Oxford: Pergamon) p 147